# Influence of geopolymer aggregates on micro-structural and durability characteristics of OPC concrete

**Article** *in* Journal of Building Pathology and Rehabilitation · December 2022

DOI: 10.1007/s41024-021-00153-y

CITATION
1

READS
76

**3 authors**, including:

Mukkala Priyanka
Vignan University
**5** PUBLICATIONS **14** CITATIONS

SEE PROFILE

Karthikeyan Muniraj
Vignan University
**18** PUBLICATIONS **149** CITATIONS

SEE PROFILE

Journal of Building Pathology and Rehabilitation (2022) 7:13
https://doi.org/10.1007/s41024-021-00153-y

RESEARCH ARTICLE

# Influence of geopolymer aggregates on micro-structural and durability characteristics of OPC concrete

**Mukkala Priyanka[1] · Karthikeyan Muniraj[1] · Sri Rama Chand Madduru[2]**

Received: 15 September 2021 / Revised: 27 November 2021 / Accepted: 27 November 2021


**Abstract**
This paper explores the physical, mechanical and durability characteristics of Fly ash—ground granulated blast furnace slag (GGBS) based Geopolymer aggregates include Specific gravity, impact value, crushing value, loss angles abrasion value, attrition value and water absorption respectively. Besides, scanning electron microscopy (SEM) was done to diagnose the microstructure of geopolymer aggregates. In addition to this mechanical, durability and microstructural behavior of the ordinary portland cement concrete made with the geopolymer aggregate includes compressive strength, split tensile strength, open porosity, water absorption, sorpitivity, Rapid Chloride Penetration Test (RCPT) and SEM with EDS were investigated. With help of SEM interfacial transition zone (ITZ) was examined. In this paper, three types of geopolymer aggregates are prepared by replacing 0, 10, and 20% of fly ash with GGBS cured under oven (at 60° for 12 h) and ambient conditions. The study considers the two grades of concrete M20 and M40 as per IS 456-2000. However, concrete prepared geopolymer Aggregates (80% fly ash and 20% GGBS) Showed higher resistance among all the tests and giving similar results at ambient and oven curing.

**Keywords** Fly ash · GGBS · Geopolymer aggregates · Mechanical properties · Durability · Microstructure

## 1 Introduction

In the present millennium, one of the principal challenges in the construction engineering is to construct structures sustainable and environmental friendly [1]. To achieve it, industrial by products like flyash, Ground Granulated Blast Furnace Slag (GGBS), red mud, metakaolin etc. came into regular utilization as cementitious materials [2–4]. Moreover, along with utilization of pozzolans, less density concrete with artificially made industrial by products based aggregates will make concrete industry more sustainable [5, 6]. Light weight aggregate concrete production and utilization have established a significant consideration in the last two decades for the structural performance [7]. The expansion in the concrete technology has permitted to make structural lightweight concrete with 100 MPa compressive strength [7, 8]. Even though, different types of lightweight aggregates are existed in the market for structural usage, there is a transformed significance in the manufacturing of flyash aggregates in the pelletization method [9, 10]. The pelletization required a technical knowledge of tilting angle, revolution speed and water content for bonding through disc pelletizer focused by Shi et al. [11]. Different studies have been carried out to examine the effect of aggregate properties on lightweight aggregate concrete [12–17]. Results indicate that the fly ash aggregates show a tough resemblance with concrete in physical, mechanical, durability, and environmental properties. Using these aggregates in the concrete can give a compressive strength up to 40 MPa [18–21]. However, to activate flyash particles water is not sufficient [22–24]; a chemical reaction is necessary to get more strength called as polymerization [25–28]. Polymerization is the action of creating tetrahedral three-dimensional chains by connecting monomers [27, 28]. The combination of silicates and hydroxides gets alkaline solution which acts as catalyst and reacts with silica and alumina in binder [29, 30]. While choosing this activator

✉ Mukkala Priyanka
Mukkala.priyanka@gmail.com

[1] Department of Civil Engineering, Vignan's Foundation for Science, Technology and Research, Vadlamudi, Guntur, AP 522213, India

[2] Department of Civil Engineering, Sree Chaitanya College of Engineering, Karimnagar, TS, India

Published online: 09 December 2021

Singh (2015) stated that sodium can release monomers from alkaline [31]. Hence the blending of sodium silicate and sodium hydroxide can be a good option for choosing an alkaline solution. Therefore, the addition of the alkaline solution in the manufacturing of Aggregates will enhance the bonding of fly ash particles. The enhanced bonding in aggregate will improve the characteristics of concrete, like compressive strength [32, 33]. In this perspective, geopolymer aggregates become one of the candidates to produce alternative aggregates for the considerations of both sustainable and environmental friendly materials. However, geopolymerization needs oven curing, which is power utilization practice [34–36], which increases the economy again. Baykal and Doven [9] stated that the engineering properties of the wet cured fly ash pellets addition of lime helps in improving the mechanical properties. However, the performance of the aggregates is not only depending on curing procedure and also the engineering properties of binder. So that GGBS can produce the necessary heat to overcome this difficulty, which can help in quick geopolymerization at ambient curing [37, 38]. GGBS is the by-product of the steel manufacturing industry, which is formed while quenching iron. The composition will change based on the raw materials in the iron production process [39].

The main objective of this paper is to know the influence of geopolymer aggregates in the durability attainment of OPC concrete. In the present study, flyash based geopolymer aggregates are manufactured by replacing 0, 10, and 20% fly ash with GGBS. The manufactured aggregates were cured under the oven and ambient curing. To study geopolymer aggregates physical properties, crushing value, impact value, abrasion value, attrition value, specific gravity, and water absorption tests were performed. In addition, the microstructural characteristics of geopolymer aggregates were studied through X-ray diffraction analysis (XRD), scanning electron microscopy (SEM), and energy dispersive X-ray spectroscopy (EDX). Besides, to understand the mechanical properties compressive strength and split tensile strength test, to examine the durability properties open porosity, water absorption, acid resistance, sorpitivity and rapid chloride penetration tests were determined for geopolymer aggregate-based concrete. However, to understand the bonding of geopolymer aggregate with cement paste the SEM analysis was conducted.

## 2 Materials and methods

In this present study, fly ash and GGBFS are used in the geopolymer aggregates production are provided from NTPS, Vijayawada, Andhra Pradesh and RINL, Visakhapatnam, Andhra Pradesh respectively conforming to ASTM 618 [40] and ASTM 989 [41]. Table 1 represents the chemical composition of the binders accordingly due to less CaO content flyash considered as Class F. It has a bulk density of 834 kg/m$^3$ and a specific surface area of 2652 cm$^2$/g, the initial and final setting times of fly ash was 356 min and 534 min, respectively. In the manufacturing of aggregates alkaline solution, a combination of sodium hydroxide and sodium silicate was used. Sodium hydroxide will be available in the form of pellets bought from Vamsi chemicals, Vijayawada. Sodium silicate was available in liquid form bought from Bhavani chemical Industries, Vijayawada, Andhra Pradesh. For the current study, sodium hydroxide solution with 8 molarity was prepared and allowed to cool about 15 min. then sodium silicate was added with a ratio of 1:2. This alkaline solution was prepared 1 day before mixing time [42–44]. $Na_2SiO_3$ to NaOH proportion is maintained as two and to ensure workability, the activator to binder ratio used for the production of aggregate is taken as 0.3. For concrete production, OPC 43 grade cement was used conforming to ASTM C 150-19 [42] fine aggregate collected from local dealers. The sieve analysis tests were carried out according to IS 2386-1963 (Part I) [43]. The result indicated that the fine aggregate is of Zone-II. Geopolymer aggregates of 12 mm, 16 mm and 20 mm sizes with the proportions of 1:1:2 are used in place of coarse aggregates. The manufacturing and properties of aggregates are discussed in the following sections.

## 3 Manufacturing of geopolymer aggregates

The geopolymer aggregates were manufactured by using a disk pelletizer. Speed of the pelletizer is maintained at 40 rotations per minute and the angle of tilt is fixed at 45°. Flyash and GGBS are added to the pelletizer and the disc was rotated for 3–5 min before adding half of the solution to the binder and continue the rotation for 3–5 min. Alkaline solution was continuously sprayed on the binder materials during the accumulation process for pellet formation which

**Table 1** Chemical composition of the binders

| Material | $Al_2O_3$ | $SiO_2$ | $Fe_2O_3$ | CaO | MgO | $Na_2O$ | $K_2O$ | MnO | $P_2O_5$ | $SO_3$ | $TiO_3$ | LOI |
|---|---|---|---|---|---|---|---|---|---|---|---|---|
| Cement | 4.08 | 21.27 | 3.17 | 65.25 | 1.98 | 0.67 | 1.02 | – | – | 1.97 | – | 0.35 |
| Fly ash | 25.10 | 58.25 | 4.6 | 2.87 | 1.2 | 0.43 | 0.86 | 2.9 | 0.15 | 1.16 | 0.83 | 1.59 |
| GGBFS | 12.14 | 1.10 | 32.22 | 45 | 4.23 | 0.82 | 0.07 | 1.92 | – | 0.85 | – | 1.99 |

is known as agglomeration [45, 46]. After forming fresh pellets, they were transferred to curing. For Ambient-cured aggregates, they were placed under a regular atmosphere under the temperature of 25 ± 2 ºC. For oven cured aggregates, they were placed in an oven chamber, at the temperature of 60 ºC for 12 h then removed from the oven and kept at ambient temperature. The formed pellets were sieved before going to testing. Figure 2 shows grading curve of the aggregates. In the laboratory scale pelletizer 20 kgs of aggregates were produced at a time. Schematic representation of the production is as shown in Fig. 1

The aggregate are sieved according to IS 2386 (Part I)—1963 [43]. Figure 2a and b shows cumulative passage of aggregates through different sieves and the gradation. The aggregates of sizes from 12 mm, 16 mm and 20 mm are used as 25%, 25%, 50% respectively. Water absorption (W) of the aggregate was calculated as per ASTM C127 [47]. It was calculated as the percentage of ratio of mass increase of aggregates after immersion in water for 24 h ($W_2$) to the dry mass of the aggregate ($W_1$) using formula $W = (W_2/W_1) \times 100$. Crushing value was calculated as the percentage ratio of amount passed from IS 2.36 sieve after crushing the aggregates at the rate of 400 kN in 10 min ($C_2$) to the initial weight of the aggregates ($C_1$) using formula $C = (C_2/C_1) \times 100$. Impact value was calculated as the percentage ratio of amount passed from IS 2.36 Sieve after giving 15 blows through impact testing machine ($I_2$) to the initial weight of the aggregates ($I_1$) using formula $I = (I_2/I_1) \times 100$. Abrasion value was calculated as the percentage ratio of amount passed from IS 1.7 mm sieve after rotating 500 rotations with 11 steel balls in the abrasion testing machine ($A_2$) to the initial weight of the aggregates ($A_1$) using formula $A = (A_2/A_1) \times 100$. Attrition value was calculated as the percentage ratio of amount passed from IS 1.7 mm Sieve after rotating 1000 rotations in the abrasion

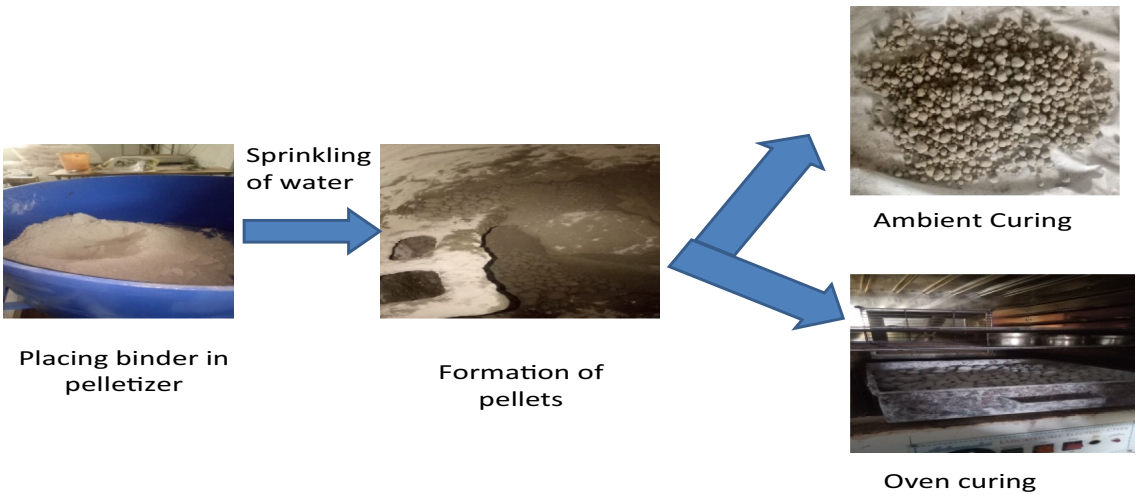


**Fig. 1** Schematic representation of process of aggregate production

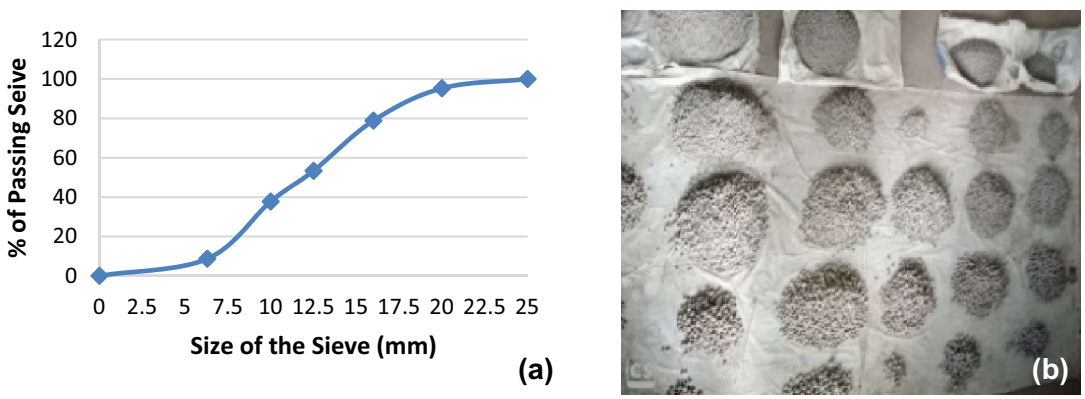


**Fig. 2** **a** Gradation curve **b** aggregates of different sizes

testing machine ($AT_2$) to the initial weight of the aggregates ($AT_1$) using formula $AT = (AT_2/AT_1) \times 100$.

## 4 Mix proportions for concrete preparations

Since the aggregates having low density the mix proportions are done in according to standard practice for selecting proportions for structural lightweight concrete ACI 211.2-98 [48]. The quantities of materials required for 1 $m^3$ volume are tabulated in Table 2. The specimens were prepared by mixing dry materials namely cement, fine aggregate and coarse aggregate initially for 5–6 min. to this the required quantity of water is added and mixed for another 3–4 min to get homogeneous mixture. After well mixing of all the materials concrete was transformed into the 150 × 150 × 150 mm moulds in three layers. Workability of the mix is calculated using slump cone test conforming to the IS 1199-1959 [49]. Total 12 different mixes were prepared by changing the aggregates proportions and curing type. Nomenclature of the mixes starts with $OF_{100}$ $G_0$ means oven cured aggregates with 100% flyash, $OF_{90}$ $G_{10}$ means oven cured aggregates with 90% flyash 10% GGBS, $OF_{80}$ $G_{20}$ means oven cured aggregates with 80% flyash GGBS 20%. Similarly $AF_{100}$ $G_0$ ambient cured aggregates with 100% flyash $AF_{90}$ $G_{10}$ means ambient cured aggregates with 90% flyash 10% GGBS, $AF_{80}$ $G_{20}$ means ambient cured aggregates with 80% flyash GGBS 20%.

After 24 h the specimens were removed from the moulds and kept in water curing for 28 days. Then compressive strength of geopolymer aggregate based concrete is found out conforming to BS EN 12390-3 [50].

## 5 Experimental program

### 5.1 Workability

Slump cone was used to test the workability of the geopolymer aggregate based concrete according to ASTM C143-15 [51]. The experiment was conducted on fresh geopolymer aggregate concrete in the laboratory with 12 different mixes changing the aggregates proportions and curing type.

### 5.2 Mechanical properties

The compressive strength test was conducted on the digital compression testing machine having maximum capacity of 2000 kN capacity with 140 kg/$cm^2$ rate of loading. The experiment is starts with the placing of specimen in the center of CTM in between two plates, continues with applying load at constant rate until the reading gets altered its direction. The ultimate failure of the specimen was indicated by reverse direction of the needle. The value is taken at the time of crack, termed as ultimate load carried by the specimen. The compressive strength of a particular specimen was determined by the ratio of ultimate load at failure of the specimen to the cross sectional area of the specimen. The specimens to test the compressive strength are cast in the sizes of 100 × 100 × 100 mm, according to the ASTM E9-19 [52]. Cylindrical samples sizes of 100 × 200 mm were cast to perform the split tensile strength which can be used to find out tensile strength of concrete indirectly. The compression testing machine was used for the test by placing the specimens in the horizontal direction according to ASTM C 496 [53].

**Table 2** Mix calculations for geopolymer aggregate concrete

| Mix | Materials | Cement (kg/$m^3$) | Silica Fume (kg/$m^3$) | Fine aggregate (kg/$m^3$) | Geopolymer aggregate (kg/$m^3$) | Water (kg/$m^3$) |
|---|---|---|---|---|---|---|
| M20 | $OF_{100}$ $G_0$ | 404 | – | 700 | 629 | 202 |
| | $OF_{90}$ $G_{10}$ | 404 | – | 700 | 629 | 202 |
| | $OF_{80}$ $G_{20}$ | 404 | – | 700 | 629 | 202 |
| | $AF_{100}$ $G_0$ | 404 | – | 700 | 629 | 202 |
| | $AF_{90}$ $G_{10}$ | 404 | – | 700 | 629 | 202 |
| | $AF_{80}$ $G_{20}$ | 404 | – | 700 | 629 | 202 |
| M40 | $OF_{100}$ $G_0$ | 450 | 43 | 596 | 644 | 202 |
| | $OF_{90}$ $G_{10}$ | 450 | 43 | 596 | 644 | 202 |
| | $OF_{80}$ $G_{20}$ | 450 | 43 | 596 | 644 | 202 |
| | $AF_{100}$ $G_0$ | 450 | 43 | 596 | 644 | 202 |
| | $AF_{90}$ $G_{10}$ | 450 | 43 | 596 | 644 | 202 |
| | $AF_{80}$ $G_{20}$ | 450 | 43 | 596 | 644 | 202 |

### 5.3 Durability properties

#### 5.3.1 Open porosity

According to ASTM 624-06 [54] open porosity experiment was carryout using 28 days water cured specimens of sizes 100 mm in diameter and 50 mm in thickness to determine the porous nature of geopolymer aggregate based concrete. The porosity was determined using the Eq. 1.

$$p = \frac{W_{ssd} - W_d}{W_{ssd} - W_w} \times 100 \tag{1}$$

where $p$ is porosity in percentage, $W_{ssd}$ is saturated surface dry weight of specimen, $W_d$ is the dry weight of the specimen, $W_w$ is wet weight of the specimen in water.

#### 5.3.2 Water absorption

According to ASTM C642-13 [55] Water absorption test was performed on the 28 days water cured specimens of sizes 100 mm in diameter and 50 mm. all the 14 specimens were kept in a oven at 105° C to assure that zero moisture content there in the concrete. Each specimen is weighed before immersing into water, after 24 h of soaking specimens were taken out as well as cleaned with a dry cloth to get rid of surface water and weighed. Using the following Eq. 2 water absorption percentage was calculated.

$$W(\%) = \frac{W_2 - W_1}{W_1} \times 100 \tag{2}$$

where $W$ percentage of water absorption, $W_1$ weight of sample before immersion and $W_2$ Weight of sample after 24 h of immersion.

#### 5.3.3 Sorptivity test

According to ASTM C 1585-13 [56] Sorptivity test was performed on the 28 days water cured specimens of sizes 100 mm in diameter and 50 mm in thickness to determine the capillary action of water through the geopolymer aggregate based concrete. It can be calculated by increase of weight of the sample at constant time. Before testing, the sample was covered by silicone gel except the one circular bottom face to make specimen impervious. The bottom face of the sample was allowed to water one centimeter above the surface of the specimen in shallow water bath. Coefficient of sorpitivity S can be calculated by considering the capillary action into count. As square root of time elapsed (t) increases the cumulative water absorption per unit area of inflow increases. The following Eq. 3 was used to calculate the sorptivity value of geopolymer aggregate based concrete.

$$S = \frac{\Delta w}{A \times d \times \sqrt{t}} \tag{3}$$

#### 5.3.4 Rapid chloride penetration test (RCPT)

According to ASTM C 1202-12 [57] Rapid chloride penetration test was performed on the 28 days water cured specimens of sizes 100 mm in diameter and 50 mm to know the electrical conductivity of geopolymer aggregate based concrete. In the equipment set up, every unit with two cells positive and negative reservoirs, positive reservoir is filled with 12 g per liter of NaOH solution and negative reservoir is filled with 30 g per liter of NaCl solution. The experiment has carried out for 6 h subjected to DC voltage of 60 V. The electricity passage between reservoirs through the sample is determined in terms of coulombs. The lowest passage of current indicates high resistance to chloride penetration.

## 6 Results and discussions

### 6.1 Characteristics of aggregates

#### 6.1.1 Physical properties of geopolymer aggregates

A comparison was made on the geopolymer aggregate properties considering the density, crushing value, impact value, specific gravity, water absorption, abrasion value, attrition value. All the tests were performed on aggregate sizes varying ranges from 6 to 12 mm. Bulk density of the Aggregates ranges from 820 to 1000 kg/m$^3$ where as conventional aggregate have 1355 kg/m$^3$, hence the aggregates comes under lightweight aggregates. Comparing the mixes, type of curing does not affected density but addition of GGBS increasing density due its higher Specific gravity and courser particle of GGBS than flyash. Water absorption and Specific gravity were tested according to the ASTM C127 [47]. The water absorption was carried out by placing a known measure of dry aggregate in a pycnometer filled with water at room temperature for a certain period of 24 h. Increased weight of surface dried aggregate was determined after removed from water. For all the six types of geopolymer aggregates water absorption varies from 7 to 11% of its weight shown in Table 3. The addition of GGBS will significantly decrease the water absorption corresponding to other two types of aggregates. Type of curing was prominently affecting water absorption since oven curing results less water absorption than

**Table 3** Physical properties of aggregates

| Type of aggregate | Crushing strength | Impact strength | Water absorption | Specific gravity | Abrasion | Attrition |
|---|---|---|---|---|---|---|
| $OF_{100}\ G_0$ | 25.84 | 26.8 | 10 | 1.89 | 15 | 12 |
| $OF_{90}\ G_{10}$ | 24.73 | 25.4 | 8 | 1.9 | 14 | 11 |
| $OF_{80}\ G_{20}$ | 20.8 | 24.7 | 7 | 1.97 | 13 | 10 |
| $AF_{100}\ G_0$ | 29.5 | 27.7 | 11 | 1.85 | 17 | 13 |
| $AF_{90}\ G_{10}$ | 27.5 | 25.7 | 10 | 1.85 | 15 | 11 |
| $AF_{80}\ G_{20}$ | 26.04 | 24.7 | 7 | 1.87 | 13 | 10 |

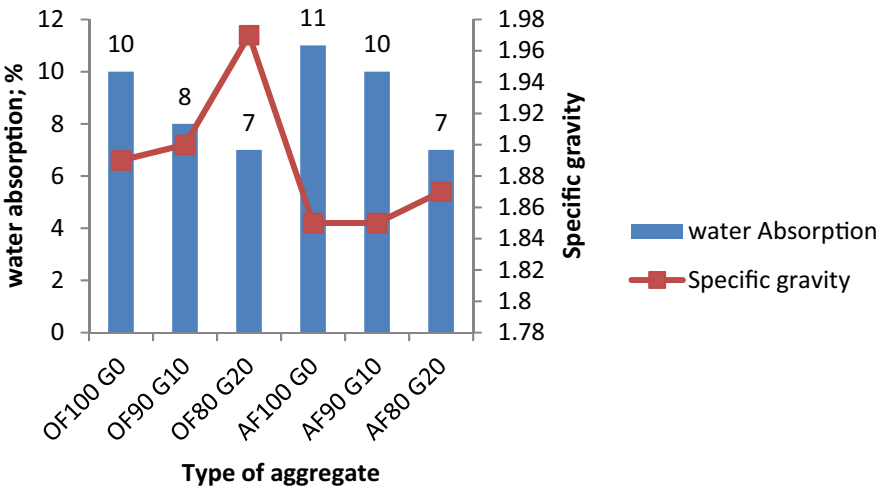


**Fig. 3** Water absorption vs specific gravity

ambient curing. Specific gravity was observed less than 2 for all the 6 types of aggregates. Maximum specific gravity 1.98 obtained at 20% GGBS with oven curing minimum is at 0% GGBS with ambient curing. Figure 3 shows graph between water absorption and specific gravity relation, similar observation was found by Jiang. The strength of lightweight aggregate was determined according to IS: 2386 (Part IV)—1963 [58] by impact value, abrasion value and attrition value. Abrasion and attrition are the resistance to rupture of material towards other and same materials. All the values are in permissible limits that are less than 30%, by observing the values in Table the addition of GGBS is enhancing the strength of aggregates due to higher calcium present in the GGBS. And also noted that ambient curing is giving equal resistance to crushing and impact with oven curing aggregates at 20% replacement of GGBS by fly ash due to heat produced at the time of geopolymerization. The same results were observed by Sarker, and Bouissi [59, 60] who found that replacement of GGBS up to 20% will increase the strength of fly ash based geopolymer paste. The aggregate imposing great resistance towards abrasion and attrition than impact and crushing due to denser medium of aggregates.

#### 6.1.2 XRD analysis of geopolymer aggregates

XRD Pattern of Ambient and oven cured Aggregates are shown in Fig. 4. It can be observed that main identifier peak is Quartz ($SiO_2$) with high intensity at $2\theta = 26°$, other than Quartz crystalline peaks absorbed are Mullite Lamite and Calcite at ambient curing with an addition Hematite and katoite at oven curing. Addition of GGBS influence the polymerization in all the six types of aggregates observe a wide bump appears between 25° and 40°. The observed amorphous peak at 35° is indicated as geopolymer Gel. Then reduction of concentration of peaks indicates that dissolution of crystalline phases of remaining materials. The literature insisting that presence of $Na_2SiO_3$ reason for reduction of crystalline phases [59, 61]

#### 6.1.3 SEM analysis of geopolymer aggregates

Images of fly ash based geopolymer aggregates varying GGBS % were shown in Fig. 5. It is evidence that all the three types of aggregates under two curing showing completely reacted matrix with no un-reacted fly ash particles. The formation of A–S–H gel was observed in each aggregate evident to good geopolymerization takes place. At 20%

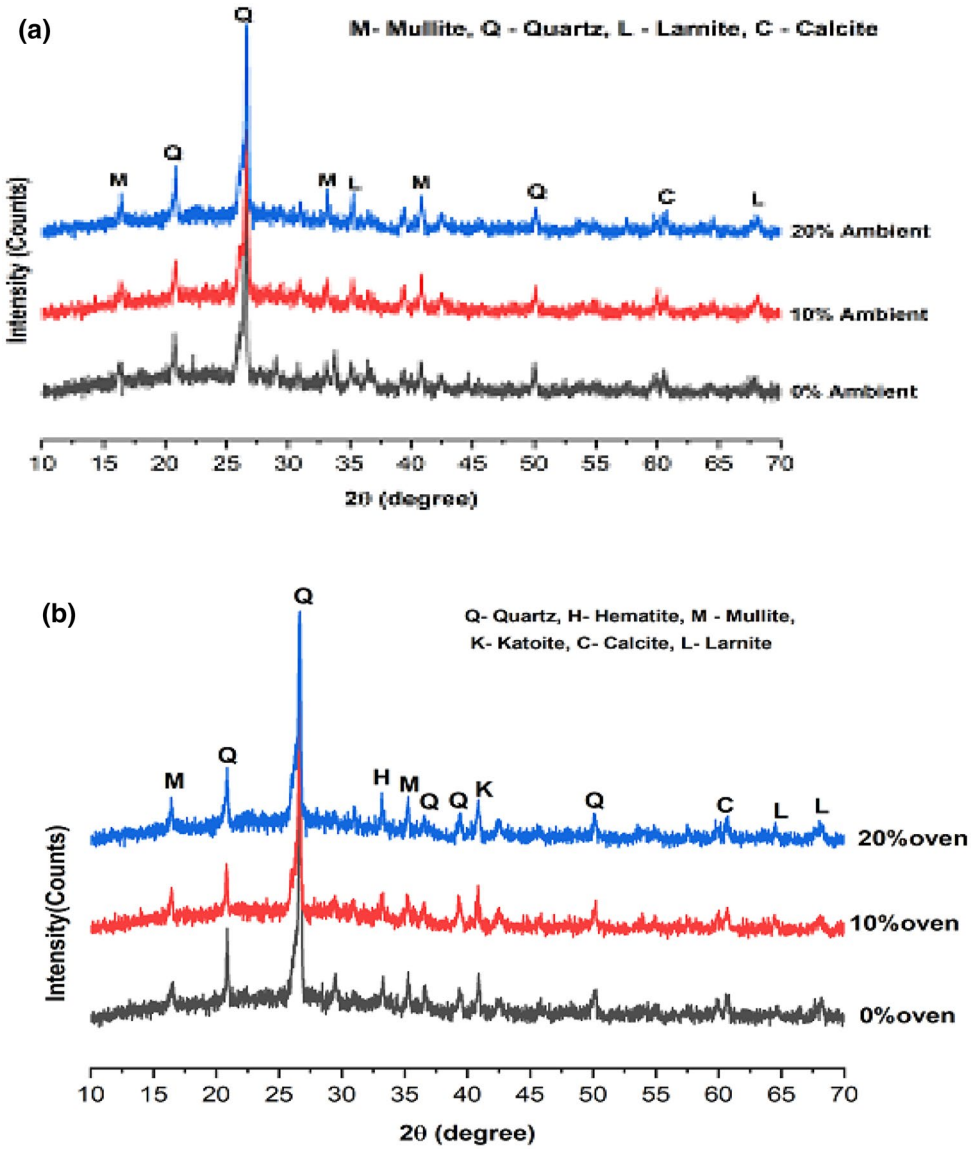


**Fig. 4** XRD pattern of **a** ambient curing **b** oven curing aggregates

replacement of GGBS shows the formation of C–A–S–H Gel due to alumina silica in the fly ash and calcium in GGBS. The clear observation notices that the micro pores in the medium of aggregates are reducing as increasing of GGBS % which is reason to get enhancing the strength properties and less water absorption. Oven curing is giving dense medium comparing with ambient curing.

## 6.2 Mechanical properties of geopolymer aggregate concrete

### 6.2.1 Workability of concrete

The workability results of fresh concrete are reported in Fig. 6. More slump value of 79 mm was observed in Mix A1 whereas mix A6 shown the lowest value 71 mm. The cause for the highest slump for mix A1 is recognized due to aggregates with no GGBS. According to the previous literature, addition of GGBS will decrease the workability of geopolymer concrete [62, 63]. In this study, when GGBS content in the Aggregates was replaced from 0 to 20%, the decreased slump values were noticed. While mix B has given less workability values compared to Mix A.

### 6.2.2 Compressive strength of concrete

Figure 7 depicts that compressive strength of concrete specimens enhancing with increase of GGBS content in the aggregates. That is to say, the compressive strength of oven cured aggregate concrete specimens after 28 days of curing (A1, A2, A3,) was 26.8, 29.2 and 30.4 MPa, respectively. Whereas, the compressive strength of remaining mixes produced with ambient cured aggregate concrete specimens gave higher values. Those values

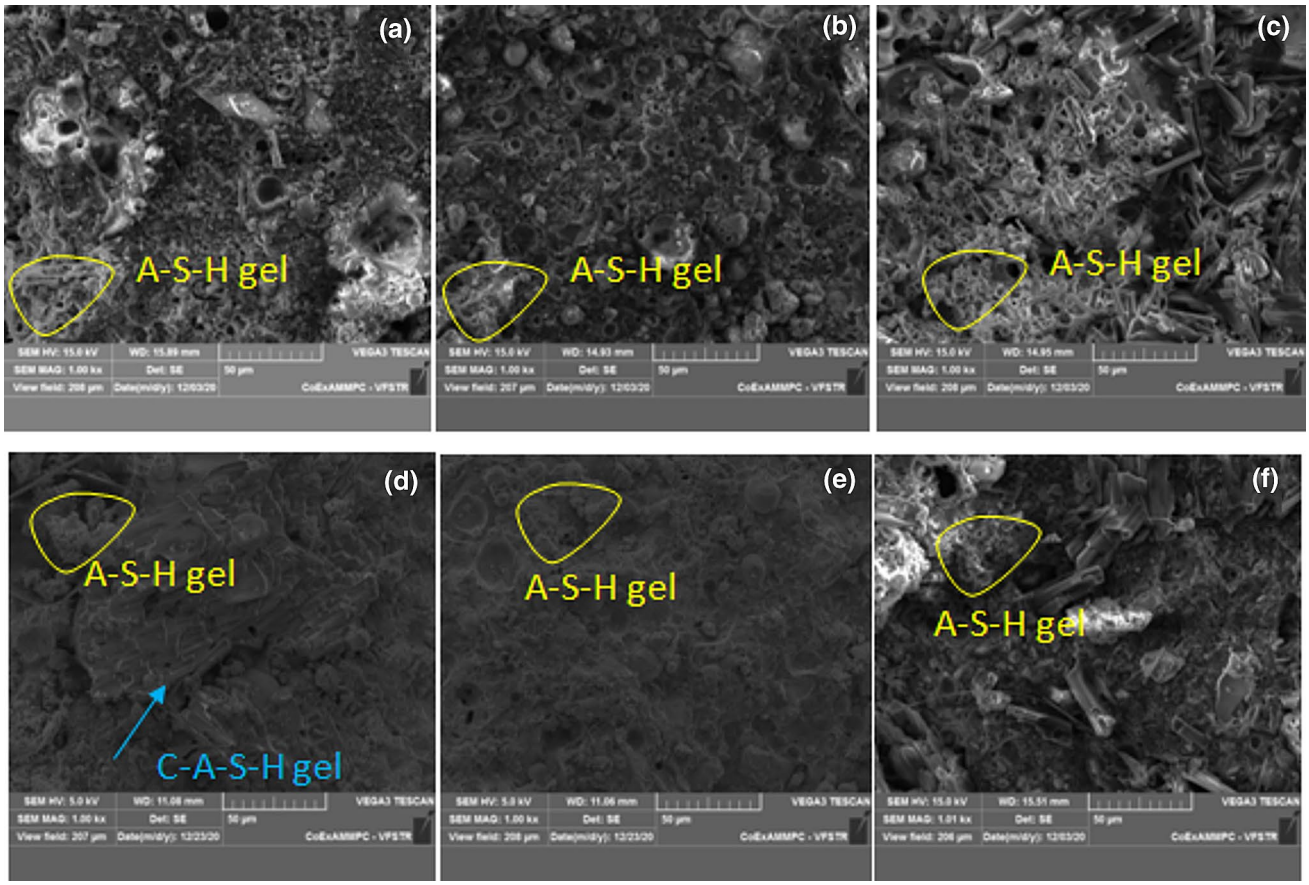


**Fig. 5** **a** 20% GGBFS at ambient curing **b** 10% GGBFS at ambient curing **c** 0% GGBFS at ambient curing **d** 20% GGBFS at oven curing **e** 10% GGBFS at oven curing **f** 0% GGBFS at oven curing

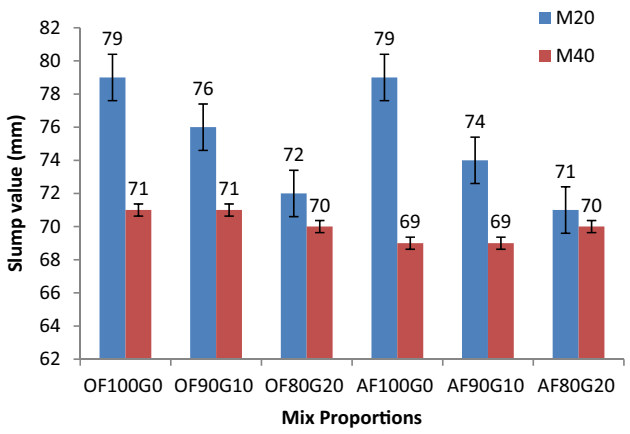


**Fig. 6** Slump cone values of fresh Geopolymer Aggregate Concrete

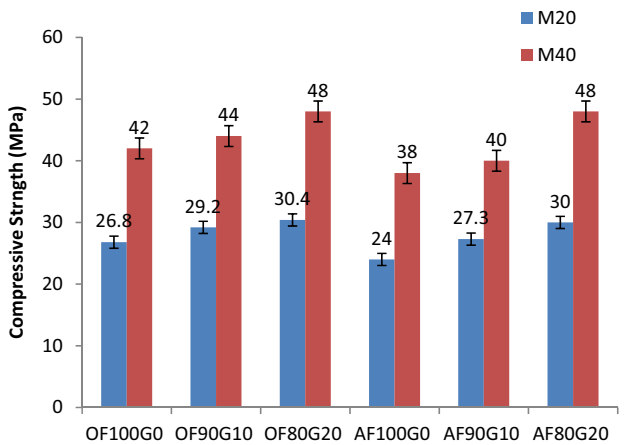


**Fig. 7** Compressive strength of geopolymer aggregate concrete

are 24, 27.3 and 30 MPa for the mixes A4, A5 and A6 respectively. Aggregates cured under oven at 60° giving more compressive strength to the concrete than ambient cured aggregates however; at 20% GGBS replaced aggregates are replicates same strength at both the curing. The Mix A3 and A6 contain 20% GGBS replaced aggregates achieved higher strength and same value at both the curing. Mix B also exposed parallel kind of results. Strength improvement in concrete is by the reason of aggregates strength which is due to the leaching of Aluminosilicates.

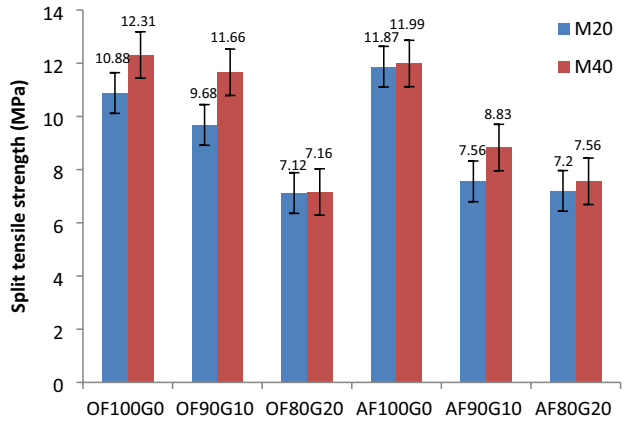


**Fig. 8** Split tensile strength of geopolymer aggregate concrete

In the process of aggregate geopolymerization, $Na^+$ ion balances the charge shortage. Moreover, the $OH^-$ ion in the alkaline solution revives the $Al^{3+}$ and $Si^{4+}$ ions from the industrial by-products and plays as catalyst [64] lower strength is due to less alkali content which slows the leaching of Aluminosilicates. In addition to this GGBS enhances the strength by producing additional C–S–H and C–A–S–H due to reaction of $Ca^+$. The enhancement in the Compressive strength was more obvious with GGBS percentage increment in the aggregates and indicates that highly reactive $Ca^+$ element.

#### 6.2.3 Split tensile strength

Figure 8 depicts 28 day split tensile strength of concrete samples using aggregates having different replacement of GGBS content. It was found that split tensile strength was enhanced from 35 to 52% in case of 20% GGBS replaced aggregate based samples at 28 days of oven curing and 26–55% in case of ambient curing. In other word split tensile strength of ambient cured aggregate concrete samples (A1, A2, and A3) was 6, 7.56, 10.68. Whereas, the Split tensile strength of oven cured aggregate concrete samples show higher values as 7.12, 9.68, 10.88 for A5, A6, A7 respectively. Similarly the strength values for M40 grade concrete mixes are 7.16, 10.99, 12.2 (B1, B2, B3) and 7.56, 11.96, 12.31 (B4, B5, B6) for ambient cured aggregate concrete samples and oven cured aggregate concrete samples correspondingly. The outcome specifies that for both mixes M20 and M40, GGBS improving the strength values. The split tensile strength values are demonstrating that the addition of GGBS quickens the geopolymerization process to attain strength of aggregates thus increase in geopolymer aggregate based concrete specimens.

### 6.3 Durability properties of geopolymer aggregate concrete

#### 6.3.1 Porosity of concrete

To understand the porosity of the geopolymer aggregate based concrete, open porosity experiment was conducted and the results were represented in Fig. 9. In mix A, reduced porosity (%) values observed from 7 (A1) to 4 (A2) at 10% GGBS replaced oven cured aggregates based concrete and 3 (A3) at 20% GGBS replaced oven cured aggregate based concrete. Similarly ambient cured aggregates based concrete shows reduction in porosity form 10 (A4) to 7.5 (A5) and 4 (A6). Mix B also reveals the parallel kind of outcomes. The concrete porosity was reduced extensively with GGBS in aggregates. It is because of void packing by C–S–H gel which is reaction Ca + in GGBS during Geopolymerization, which is noticed in the microstructural examination in the current research (represented at "SEM–EDS analysis"). Furthermore, fineness of GGBS was the another reason, which fill up the void structure of aggregates hence less pores in concrete. Dense structured aggregates were formed due to fineness of GGBS, which reduces concrete porosity.

#### 6.3.2 Water absorption of concrete

The water absorption test was conducted after 28 days of curing. The contemplation of curiosity is to recognize the resistance of water absorption in Geopolymer aggregate based concrete with GGBS replacement with oven and ambient curing. Figure 10 illustrates that the percentage of water absorption of concrete at various GGBS replaced aggregates with oven and ambient curing. For GGBS replaced oven cured aggregates concrete, water absorption reduced from 4.2% (A1) to 4% (A2) and 3.73% (A3) at 10 and 20 percentage replacements respectively. Similarly for ambient cured aggregates concrete the reduction was from 5.56%

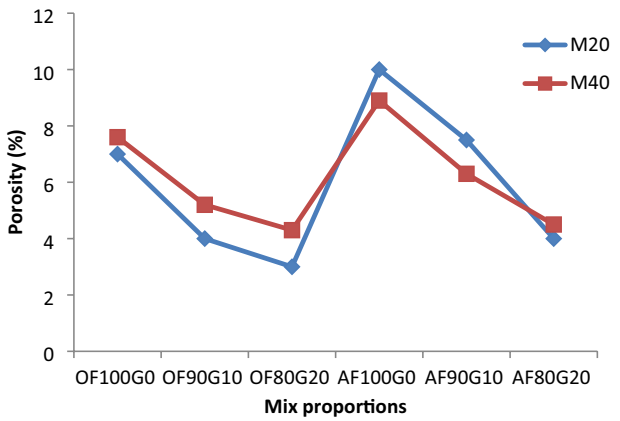


**Fig. 9** Porosity results of geopolymer aggregate concrete

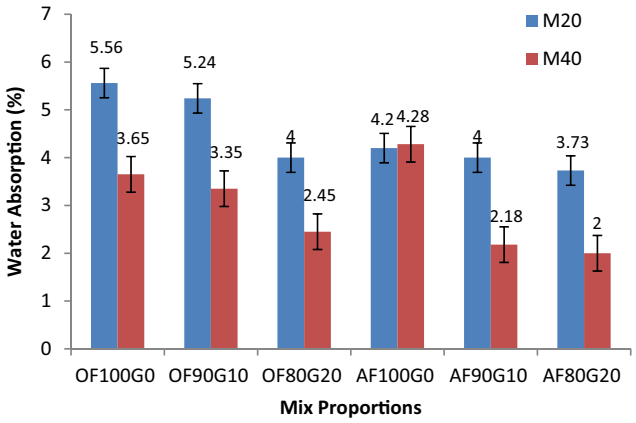


**Fig. 10** Water absorption values of geopolymer aggregate concrete

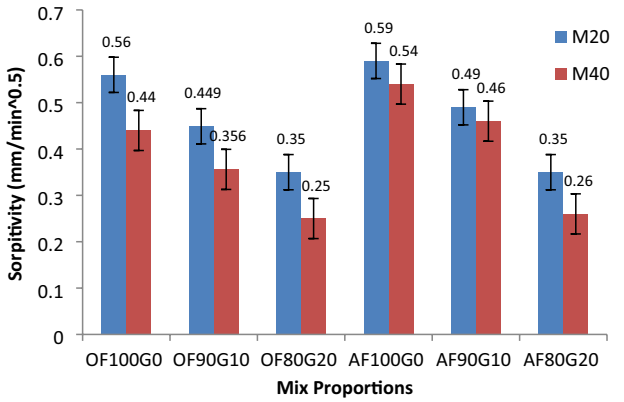


**Fig. 11** Sorpitivity values of geopolymer aggregate concrete

(A4) to 5.24% (A5) and 4% (A6) respectively. However in case of mix B water absorption reduced from 3.65% (B1) to 3.3% (B2) then 2% (B3) at oven cured aggregates concrete and 4,28% (B4) to 2.48% (B5) then 2.18% (B6) at ambient cured aggregate concrete. The results demonstrate that with oven curing and with enhanced replacement level of GGBS, reduced water absorption values were observed. GGBS blossoms the pozzolanic action after long age also; which leads to diminishing connection between voids. An added reason for increasing in resistance towards water absorption is the fineness of GGBS particles (average particle size 9.2 µm); hence sealed all the pores and micro cracks present in the aggregates leads less pores in concrete. Large specific Surface area of GGBS can reduce the water absorption of Aggregates. A similar reason given by Manifroi in 2014; in the GGBS-based geopolymerization process, the more $Ca(OH)_2$ crystals were splits as numerous tiny crystals and less oriented, which leads to reducing of pore links leads less water absorption.

### 6.3.3 Sorpitivity of concrete

It is clear from Fig. 11. that geopolymer concrete has less water sorpitivity, followed by geopolymer based aggregate concrete. Present data indicated that the capillary action of oven cured aggregate based concrete samples transport less water than ambient cured aggregate based. This recognizable fact reveals that Geopolymer aggregate based concrete is good durable in conditions of water allowance. Though, it was noted that replacement of GGBS in geopolymer aggregate improved the performance of microstructure, which can resist water absorption, porosity and sorpitivity. The sorptivity results for mix A concrete contains oven and ambient cured aggregate are 0.56 (A1), 0.45 (A2), 0.35 (A3) and 0.59 (A4), 0.49 (A5), 0.35 (A6) respectively. Whereas the sorpitivity values for Mix B concrete contains oven and ambient cured aggregate are 0.44 (B1), 0.35 (B2), 0.25 (B3) and 0.54 (B4), 0.46 (B5), 0.26 (B6) respectively.

### 6.3.4 Rapid chloride penetration test for concrete

To determine the electrical conductivity of concrete, RCPT is a basic test which associates with pore structure and chemistry of cement paste [65]. In the present study, the passage of chloride ions into geopolymer aggregate based concrete was investigated according to ASTM C1202-19 [57], Fig. 12 represents the total charge accepted in M20 and M40 grade concrete samples with aggregates replaced with different GGBS percentages with oven and ambient curing. According to ASTM a very low and moderate chloride penetrated concrete will allow a charge of less than 1000 and 4000 coulombs respectively [66]. Since geopolymer aggregate having presence of alkaline solution which is greatly conductive and needs good geopolymerization of at least 28 days before casting concrete specimens. As per experimental data, increasing in GGBS replacement results the reduction of chlorides passage from 2050 C (A1) to 1653 C (A2) and

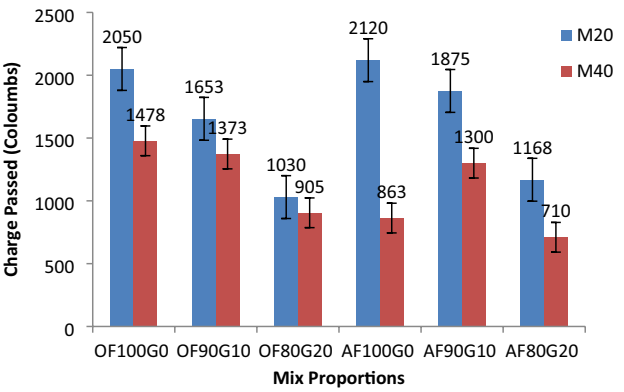


**Fig. 12** RCPT values of geopolymer aggregate concrete

1030 C (A3) in case of oven cured aggregate concrete. Similarly for series mix B, the charge values are 1373C (B1), 905C (B2), 710C (B3) and 1478C (B4), 1300C (B5), 863C (B6) for oven and ambient cured aggregate based concrete respectively. For both the mixes 20% GGBS replaced and oven cured aggregate concrete samples are resisting chlorides moderately than the other samples. The C–S–H gel decreases the majority of the pores and GGBS particles fill some more voids in the aggregates which minimizing the chloride ion penetration of concrete. Most of the researchers reported that fineness of GGBS particles reduces the chloride ion penetration and carbonation depth as in this study.

### 6.4 Micro-structural analysis of geopolymer aggregate concrete

#### 6.4.1 Interfacial transition zone (ITZ)

Figure 13 represents the images of microstructure with 20% of GGBS Aggregate concrete under ambient and oven curing, gives morphological characteristics. Aggregates are completely packed with neighboring cement matrix, this would be the cause for the constraint of micro-cracks and voids. Interfacial Transition Zone (ITZ) was alleged to be a weaker zone in the concrete mix, from the observations it is noted that the micro difference between cement matrix and aggregate are termed as micro- hardness number and it was less than 10 micro meters for the two samples hence which is having high-bonding nature where as in Jiang [67] got 30 micron meters.

#### 6.4.2 SEM analysis of geopolymer aggregate concrete

Figure 14a, b represents the hydration phase of concrete after 28 days of curing containing 20% of GGBS Aggregate under ambient and oven curing; here, calcium silicate hydrate(C–S–H) and calcium hydroxide formations are observed in both the mixes. There are no unreacted cement particles in the concrete mixes. Very minute cracks are observed and medium of the concrete seems as very denser without pores. Therefore it is the reason for getting highest strength than the other samples.

#### 6.4.3 EDX analysis of geopolymer aggregate concrete

Figure 15 addresses energy dispersive X-ray spectroscopy values for the equivalent blends. Table 4 shows the basic elemental composition in weight %, three spots are chosen on each example as displayed in Fig. 16 and normal of three spots basic weight rates are referenced in particular table which are affirmed that both blends had stable C–S–H gel arrangement. The Ca/Si of oven and ambient curing are 1.56 and 1.82. By and large, if the Ca/Si goes from 0.85 to 2.4, it is proof of C–S–H gel arrangement. Lower Ca/Si shows higher C–S–H gel arrangement [68, 69]. In the current examination, microstructure investigation uncovered that enhancement of mechanical strength is due to good strength of aggregates, bond between aggregates and cement matrix.

## 7 Conclusions

Following are the conclusions strained based on the experimental Investigation of concrete made with flyash GGBS based geopolymer aggregate.

- The aggregate prosing to utilize in the construction since all the tested values are in permissible limits and imposing immense resistance with respect to abrasion and attrition than impact and crushing due to denser medium of aggregates. The highest water absorption percentage of the aggregates is 11 which less than 12% hence can be used for the construction excluding water retaining structures.
- The replacement of GGBS in Flyash-based Geopolymer Aggregates concrete found enhancement in mechanical Characteristics. The reduction in porosity, Sorpitivity, water absorption, and corresponding improvement in the compressive strength as a result of the more C–A–S–H gel formation, which enhanced the microstructural Characteristics.
- The improved mechanical characteristics of the Flyash based geopolymer aggregate concrete specimens were found with the expansion of GGBS content because of the development of C–A–S–H gel which assists to form aggregates in denser structure and gives higher strength to the concrete. The higher strength esteems were achieved at 20% of flyash replacement by GGBS.
- The compressive strength attained at 20% replacement of GGBS giving an equal strength (25 MPa) at both the curing conditions hence to avoid oven curing 20% GGBS replacement will assist.
- SEM, EDS, and XRD images of fly ash-GGBS-based geopolymer aggregate concrete samples shown better microstructural behavior because of superior Hydration process.
- The experimental values are proving that geopolymer aggregates has enough ability to replace those conventional aggregates in some of civil engineering works

The future extent of the work is the sustainable advancement of fly ash-GGBS-based geopolymer aggregate concrete in the realistic construction applications in possible areas.

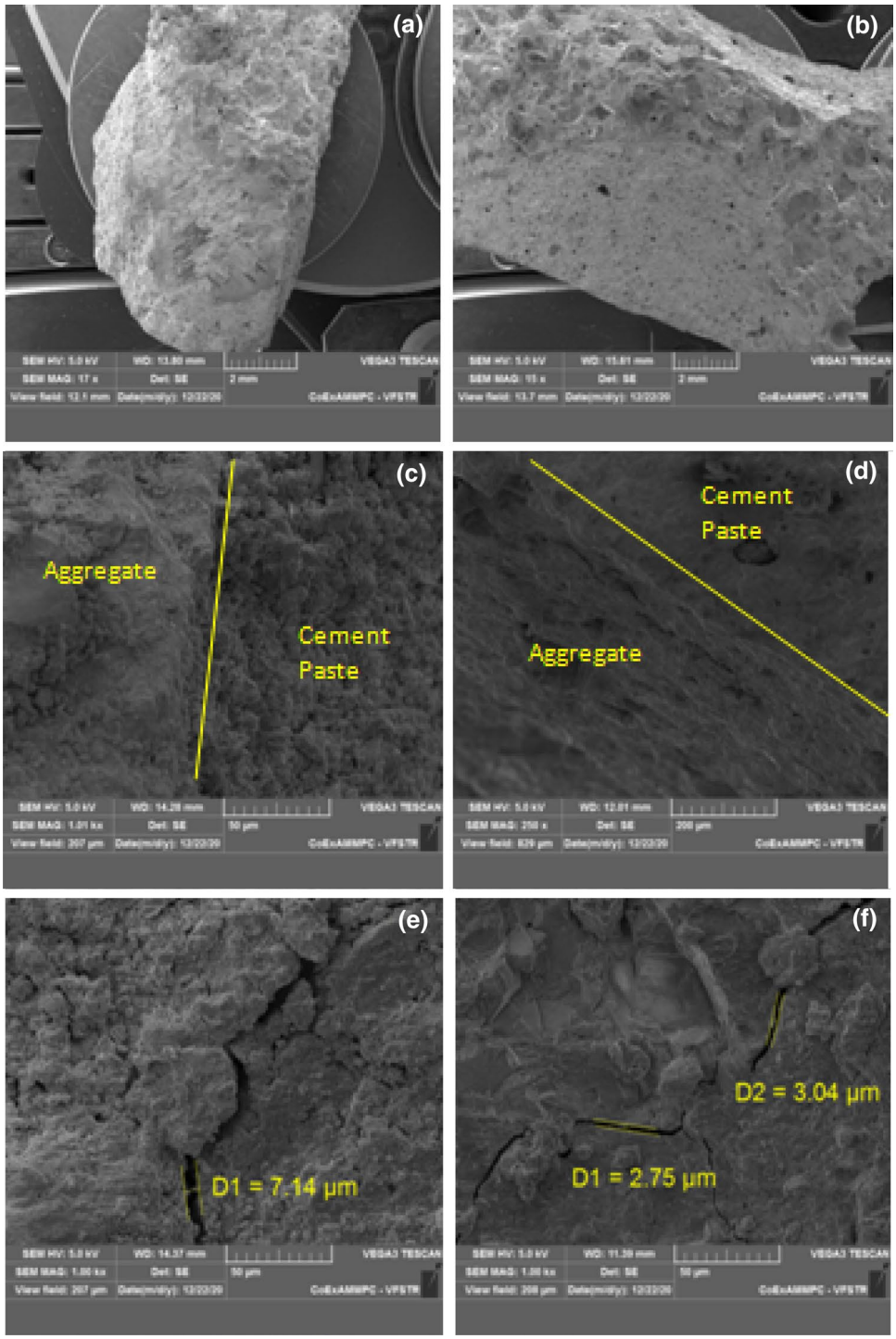


**Fig. 13** SEM images, **a** external surface ambient curing, **b** external surface oven curing, **c** internal structure ambient curing, **d** internal structure oven curing, **e** hardness number at ambient curing, **f** hardness number at oven curing

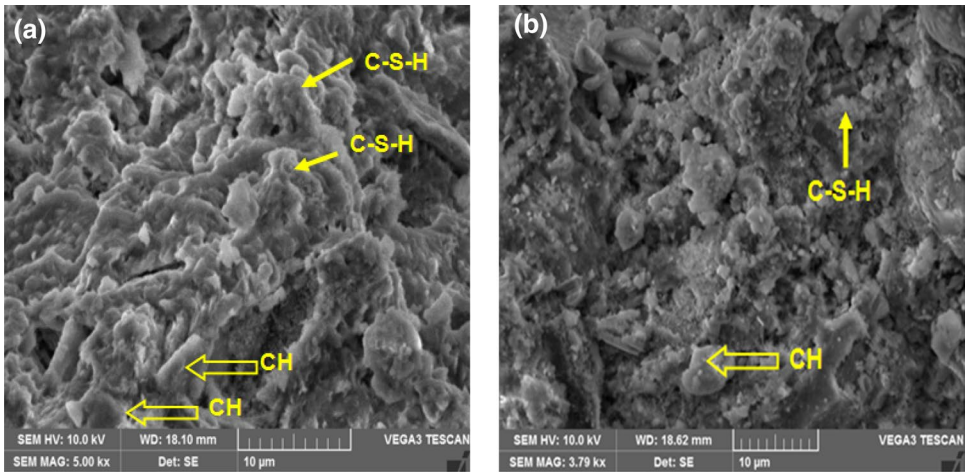


**Fig. 14** Scanning electron microscopy image for **a** ambient curing aggregate concrete and **b** oven curing aggregates concrete

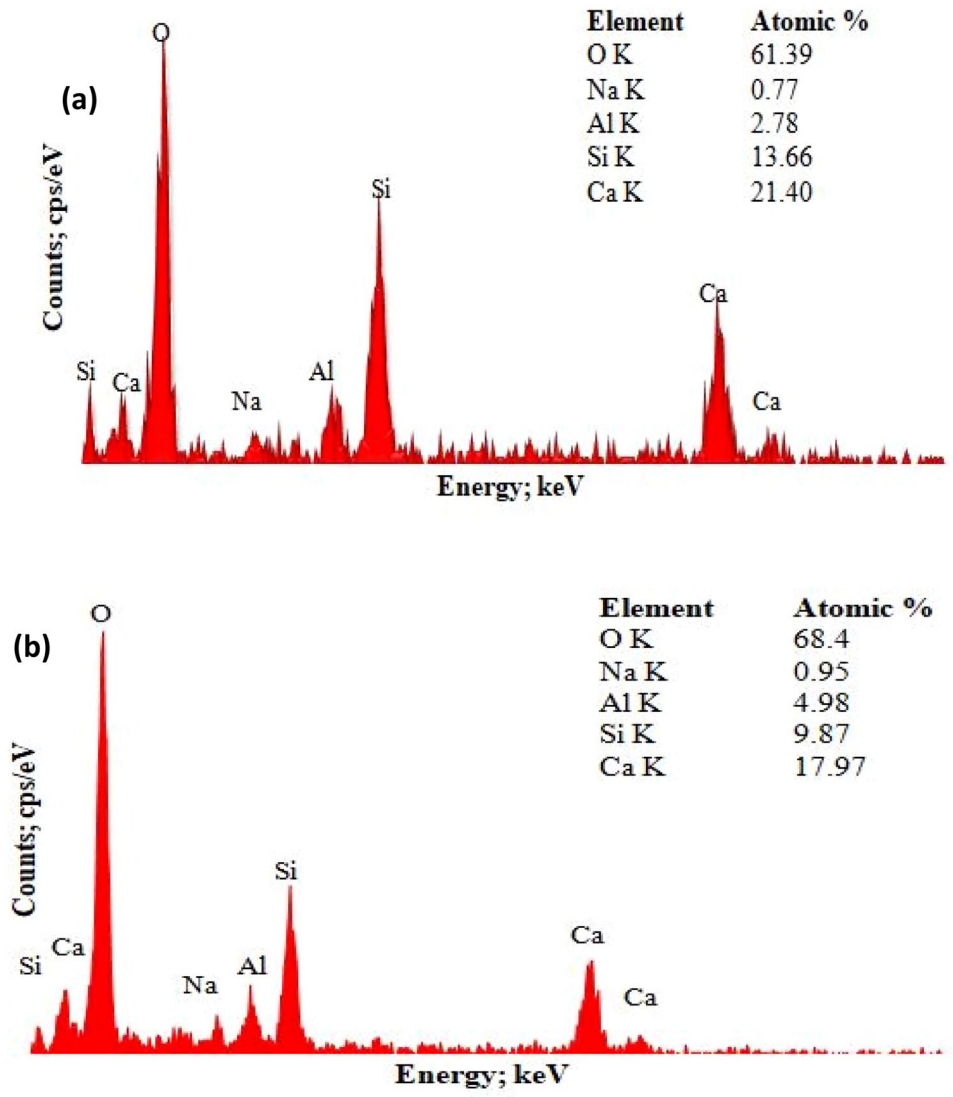


**Fig. 15** Energy dispersive spectroscopy analysis for **a** ambient curing aggregate concrete and **b** oven curing aggregate concrete

**Table 4** Energy dispersive spectroscopy results

| Mix | OK | NaK | AlK | SiK | CaK | Ca/Si |
|---|---|---|---|---|---|---|
| $AF_{80}\ G_{20}$ | 61.39 | 0.77 | 2.78 | 13.66 | 21.40 | 1.56 |
| $OF_{80}\ G_{20}$ | 68.4 | 0.95 | 4.98 | 9.87 | 17.97 | 1.82 |

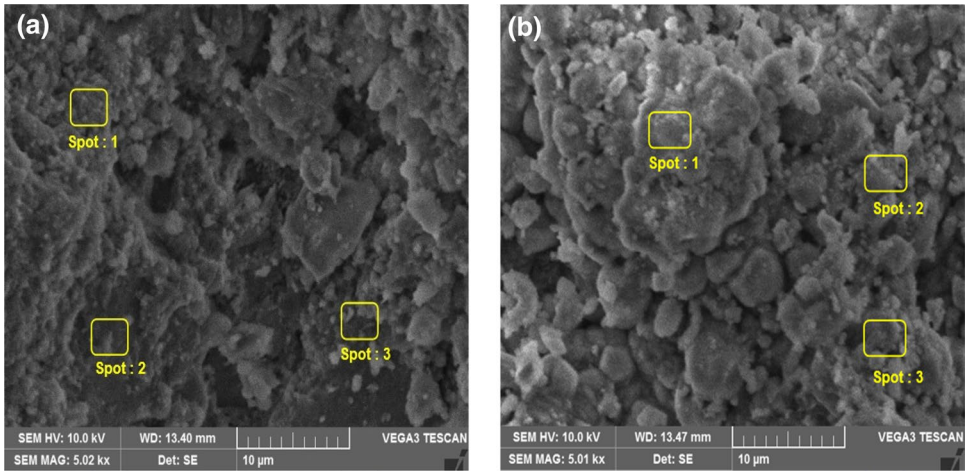


**Fig. 16** Energy dispersive spectroscopy analysis spots for **a** ambient curing aggregate concrete and **b** oven curing aggregate concrete

## Declarations

**Conflict of interest** The authors declare that they have no conflict of interest.

## References


1. Gesoğlu M, Özturan T, Güneyisi E (2007) Effects of fly ash properties on characteristics of cold-bonded fly ash lightweight aggregates. Constr Build Mater 21(9):1869–1878
2. Venkatesh C, Nerella R, Chand MSR (2020) Experimental investigation of strength, durability, and microstructure of red-mud concrete. J Korean Ceram Soc 57(2):167–174
3. Bellum RR, Muniraj K, Madduru SRC (2020) Influence of slag on mechanical and durability properties of fly ash-based geopolymer concrete. J Korean Ceram Soc 57:530–545
4. Suresh GV, Karthikeyan J (2016) Performance enhancement of green concrete. In: Proceedings of the Institution of Civil Engineers-Engineering Sustainability, vol. 171. No. 4. Thomas Telford Ltd
5. Haque MN, AI-Khaiat H, Kayali O (2002) Structural lightweight concrete–an environmentally responsible material of construction. In: Challenges of Concrete Construction: Volume 5, Sustainable Concrete Construction: Proceedings of the International Conference held at the University of Dundee, Scotland, UK on 9–11 September 2002. Thomas Telford Publishing
6. Bremner TW (1998) Lightweight concrete—an environmentally friendly material
7. Zhang MH, Gjvorv OE (1991) Mechanical properties of high-strength lightweight concrete. Mater J 88(3):240–247
8. Khaloo AR, Kim N (1999) Effect of curing condition on strength and elastic modulus of lightweight high-strength concrete. Mater J 96(4):485–490
9. Baykal G, Döven AG (2000) Utilization of fly ash by pelletization process; theory, application areas and research results. Resour Conserv Recycl 30(1):59–77
10. Döven AG (1998) Lightweight fly ash aggregate production using cold bonding agglomeration process. Diss. PhD Thesis, Boğaziçi University, İstanbul, Türkiye
11. Shi M et al (2019) Turning concrete waste powder into carbonated artificial aggregates. Constr Build Mater 199:178–184
12. Chen HJ et al (1999) Determination of the dividing strength and its relation to the concrete strength in lightweight aggregate concrete. Cement Concr Compos 21(1):29–37
13. Videla C, Lo M (2000) Mixture proportioning methodology for structural sand-lightweight concrete. Mater J 97(3):281–289
14. Zhang M-H, Gjorv OddE (1991) Characteristics of lightweight aggregates for high-strength concrete. Mater J 88(2):150–158
15. Swamy RN, Lambert GH (1981) The microstructure of Lytag aggregate. Int J Cem Compos Lightweight Concr 3(4):273–282
16. Wasserman R, Bentur A (1997) Effect of lightweight fly ash aggregate microstructure on the strength of concretes. Cem Concr Res 27(4):525–537
17. Wasserman R, Bentur A (1996) Interfacial interactions in lightweight aggregate concretes and their influence on the concrete strength. Cement Concr Compos 18(1):67–76
18. Chang T-P, Shieh M-M (1996) Fracture properties of lightweight concrete. Cem Concr Res 26(2):181–188
19. Yang C-C (1997) Approximate elastic moduli of lightweight aggregate. Cem Concr Res 27(7):1021–1030
20. Chi JM et al (2003) Effect of aggregate properties on the strength and stiffness of lightweight concrete. Cement Concr Compos 25(2):197–205
21. Gesoğlu M, Özturan T, Güneyisi E (2004) Shrinkage cracking of lightweight concrete made with cold-bonded fly ash aggregates. Cem Concr Res 34(7):1121–1130
22. Palomo A, Grutzeck MW, Blanco MT (1999) Alkali-activated fly ashes: a cement for the future. Cement Concr Res 29(8):1323–1329
23. Hardjito D et al (2004) On the development of fly ash-based geopolymer concrete. Mater J 101(6):467–472

24. Davidovits J (1991) Geopolymers: inorganic polymeric new materials. J Therm Anal Calorim 37(8):1633–1656
25. Davidovits, Joseph. Geopolymer chemistry and applications. Geopolymer Institute, 2008.
26. Yang K-H, Song J-K, Song K-I (2013) Assessment of $CO_2$ reduction of alkali-activated concrete. J Clean Prod 39:265–272
27. Shaikh FUA (2016) Mechanical and durability properties of fly ash geopolymer concrete containing recycled coarse aggregates. Int J Sustain Built Environ 5(2):277–287
28. Diaz EI, Allouche EN, Eklund S (2010) Factors affecting the suitability of fly ash as source material for geopolymers. Fuel 89:992–996
29. Yip CK et al (2008) Effect of calcium silicate sources on geopolymerisation. Cement Concr Res 38(4):554–564
30. Scrivener KL, Crumbie AK, Laugesen P (2004) The interfacial transition zone (ITZ) between cement paste and aggregate in concrete. Interface Sci 12(4):411–421
31. Singh B et al (2015) Geopolymer concrete: a review of some recent developments. Constr Build Mater 85:78–90
32. Scrivener KL, Cabiron J-L, Letourneux R (1999) High-performance concretes from calcium aluminate cements. Cem Concr Res 29(8):1215–1223
33. Ardalan RB et al (2017) Enhancing the permeability and abrasion resistance of concrete using colloidal nano-$SiO_2$ oxide and spraying nanosilicon practices. Constr Build Mater 146:128–135
34. Nagalia G et al (2016) Compressive strength and microstructural properties of fly ash–based geopolymer concrete. J Mater Civ Eng 28(12):04016144
35. Valencia S, Gustavo W, Angulo DE, de Gutiérrez RM (2016) Fly ash slag geopolymer concrete: resistance to sodium and magnesium sulfate attack. J Mater Civ Eng 28(12):04016148
36. Gunasekera C, Setunge S, Law DW (2017) Correlations between mechanical properties of low-calcium fly ash geopolymer concretes. J Mater Civ Eng 29(9):04017111
37. Bellum RR et al (2020) Investigation on performance enhancement of fly ash-GGBFS based graphene geopolymer concrete. J Build Eng 32:101659
38. Rao GM, Gunneswara-Rao TD (2015) Final setting time and compressive strength of fly ash and GGBS-based geopolymer paste and mortar. Arab J Sci Eng 40(11):3067–3074
39. Shahmansouri AA, Bengar HA, Ghanbari S (2020) Compressive strength prediction of eco-efficient GGBS-based geopolymer concrete using GEP method. J Build Eng 31:101326
40. ASTM C618-19 (2019) Standard specification for coal fly ash and raw or calcined natural pozzolan for use in concrete, ASTM International, West Conshohocken, PA, www.astm.org
41. ASTM C989/C989M-18a (2018) Standard specification for slag cement for use in concrete and mortars, ASTM International, West Conshohocken, PA, www.astm.org
42. ASTM C150, C150M-19a (2019) Standard specification for Portland cement. ASTM International, West Conshohocken
43. IS 2386-1 (1963): Methods of test for aggregates for concrete, part i: particle size and shape [CED 2: Cement and Concrete].
44. Aydin E, Arel HŞ (2017) Characterization of high-volume fly-ash cement pastes for sustainable construction applications. Constr Build Mater 157:96–107
45. Yousuf A et al (2020) Fly ash: production and utilization in India-an overview. J Mater Environ Sci 11(6):911–921
46. Aydın E (2009) Utilization of high volume fly ash cement paste in civil engineering construction sites. In: Fifth International Conference on Construction in the 21st Century
47. ASTM C127-15 (2015) Standard test method for relative density (specific gravity) and absorption of coarse aggregate, ASTM International, West Conshohocken, PA, www.astm.org
48. ACI 211.2-98 ACI standard practice for selecting proportions for structural lightweight concrete
49. IS 1199 (1959): Methods of sampling and analysis of concrete [CED 2: Cement and Concrete]
50. BS EN 12390-3:2019—TC tracked changes. Testing hardened concrete. Compressive strength of test specimens
51. ASTM C143/C143M (1998) Standard test method for slump of hydraulic—cement concrete. STM International, West Conshohocken
52. ASTM E9-19, Standard Test methods of compression testing of metallic materials at room temperature. American Society for Testing and Materials
53. ASTM C496/C496M-17, Standard test method for splitting tensile strength of cylindrical concrete specimens. American Society for Testing and Materials
54. ASTM C 642-06 (2006) Standard test method for density, absorption and voids in hardened concrete. ASTM International, West Conshohocken, PA
55. ASTM C642-13, Standard test method for density, absorption, and voids in hardened concrete
56. ASTM C 1585:2013, Standard test method for measurement of rate of absorption of water by hydraulic-cement concretes
57. ASTM C1202-19, Standard test method for electrical indication of concrete's ability to resist chloride ion penetration
58. IS 2386-4 (1963) Methods of test for aggregates for concrete, part 4: mechanical properties [CED 2: Cement and Concrete]
59. Bouaissi A et al (2019) Mechanical properties and microstructure analysis of FA-GGBS-HMNS based geopolymer concrete. Constr Build Mater 210:198–209
60. Sarkar SL, Satish C, Leif B (1992) Interdependence of microstructure and strength of structural lightweight aggregate concrete. Cement Concr Compos 14(4):239–248
61. Chindaprasirt P et al (2011) High-strength geopolymer using fine high-calcium fly ash. J Mater Civ Eng 23(3):264–270
62. Deb PS, Nath P, Sarker PK (2014) The effects of ground granulated blast-furnace slag blending with FA and activator content on the workability and strength properties of geopolymer concrete cured at ambient temperature. Mater Des 62:32–39. https://doi.org/10.1016/j.matdes.2014.05.001
63. Nath P, Sarker PK (2014) Effect of GGBFS on setting, workability and early strength properties of FA geopolymer concrete cured in ambient condition. Constr Build Mater 66:163
64. Marjanovic M, Komljenovic Z, Baacarević V, Nikolic R (2015) Petrovic, Physical–mechanical and microstructural propertiesof alkaliactivated fly ash–blast furnace slag blends. Ceram Int 41(1):1421–1435
65. Shi C (2004) Effect of mixing proportions of concrete on its electrical conductivity and the rapid chloride permeability test (ASTM C1202 or ASSHTO T277) Results. Cem Concr Res 34:537–545
66. Arup H, Sorensen B, Frederiksen J, Thuaulow N. The rapid chloride penetration test-an assessment, NACE corrosion-93, New Orleans, LA, March, pp 7–12
67. Jiang Y, Ling T-C, Shi M (2020) Strength enhancement of artificial aggregate prepared with waste concrete powder and its impact on concrete properties. J Clean Prod 257:120515
68. Rossignolo JA (2009) Interfacial interactions in concretes with silica fume and SBR latex. Constr Build Mater 23(2):817–821
69. Madduru SRC et al (2018) Performance and microstructure characteristics of self-curing self-compacting concrete. Adv Cement Res 30(10):451–468
70. Davidovits J et al (1999) Geopolymeric cement based on low cost geologic materials. Results from the European research project geocistem. In: Proceedings of the 2nd International Conference on Geopolymer, vol. 99

71. Manfroi EP, Cheriaf M, Rocha JC (2014) Microstructure, mineralogy and environmental evaluation of cementitious composites produced with red mud waste. Constr Build Mater 67:29–36